Journal of Hydrology 624 (2023) 129886

Contents lists available at ScienceDirect

Journal of Hydrology

journal homepage: www.elsevier.com/locate/jhydrol

Research papers

Modeling rainfall-driven transport of Glyphosate in the vadose zone of two experimental sites in North-East Italy

Leonardo Costa [a,*], Marta Mencaroni [b], Nicola Dal Ferro [b], Alessandra Cardinali [b], Matteo Camporese [a], Francesco Morari [b], Giuseppe Zanin [b], Paolo Salandin [a]

[a] Department of Civil, Environmental and Architectural Engineering, University of Padova, Via Marzolo 9, 35131 Padova, Italy
[b] Department of Agronomy, Food, Natural resources, Animals and Environment, Agripolis, University of Padova, Viale Dell'Università 16, 35020 Legnaro (Padova), Italy

ARTICLE INFO

This manuscript was handled by Yuefei Huang, Editor-in-Chief, with the assistance of Diederik Jacques, Associate Editor.

Keywords:
Unsaturated soil
Pesticides
Glyphosate
Infiltration

ABSTRACT

A vertical one-dimensional analysis of infiltration processes and mobility of a tracer (potassium bromide) and a glyphosate-based herbicide, both subjected to hydrological forcing, was performed. Glyphosate is a widespread herbicide whose potential harmfulness and mobility under hydrological forcing have not been fully understood yet. Here, the spatio-temporal evolution of the two compounds was monitored for one year in two experimental sites (Settolo - Valdobbiadene, Colnù - Conegliano), located within the production area of the Prosecco wine (Treviso, Italy). In each experimental site the activities were carried out on two 25 m^2 plots located at distances of 50-100 m from each other. The interpretative analyses considered rainwater infiltration as the driving mechanism of the herbicide transport and allowed us to obtain the calibration of a one-dimensional hydrologic model in each monitored plot. Different scenarios of the tracer evolution were simulated considering the pedologic properties of the shallower soil layers, the status of the plant coverage and of the root apparati, leading to a satisfactory reproduction of the observations in both the experimental sites. Modeling the mobility of the herbicide, considering also the degradation to its metabolite AMPA, proved to be more challenging, due to the tendency of glyphosate to be adsorbed to the soil matrix rather than be dissolved in water and transported toward deeper soil layers. Nevertheless, the analysis of model results for tracer and herbicide, compared with in situ observations, suggests that the transport of the glyphosate can take place even when it is adsorbed to the soil, through the movement, triggered by intense precipitation events, of microscopic soil particles within preferential flow paths.

1. Introduction

Agricultural practices in areas where groundwater is exploited for drinking water supply can impact water quality, due to the widespread use of plant protection products (PPPs). A vivid example can be found in north-eastern Italy, where a combination of agricultural practices and other anthropogenic activities (Dal Ferro et al., 2016) are carried out within wellhead protection areas in a highly urbanized territory. In the piedmont area of this region, favorable soil and climate conditions for the Prosecco wine production and abundance of good-quality water from shallower unconfined aquifers, have pushed the grape cultivation and the extraction of drinking water to coexist. The production of this typical wine increased in a decade from 60 million bottles to 92.1 million bottles per year. This caused an increase of land cover for vineyards and a larger use of plant protection products. Nowadays, the wine is produced harvesting the grape grown in a hilly area of 8400 hectares. This portion of the Veneto Region, named hills of Prosecco (Fig. 1), is classified through the italian protected designation of origin label "Denomination of Controlled and Guaranteed Origin" (DOCG in italian) and it is recognized as a UNESCO heritage. In 2019, the use of PPPs has reached 10.4 million units (liters or kilograms depending on the pesticides formulation) in the province of Treviso (Veneto, Italy) (data from ARPAV, 2020). Among these, 910,000 units (approximately 10%) were used in the grape cultivation for the Prosecco production. The use of PPPs has raised concerns about the possibility that active ingredients may infiltrate the soil and reach the aquifers exploited for drinking water supply (e.g., Costa and Salandin, 2022). Among others, the N-(phosphonomethyl)glycine, commonly known as glyphosate (GLP), one of the most widely applied herbicides since the 1980s, has raised concerns about its potential movement to groundwater (Mencaroni et al., 2023) and harmfulness (Leon et al., 2019; International Agency for Research on Cancer, 2017). This fact is of absolute relevance considering

* Corresponding author.
E-mail address: leonardo.costa@unipd.it (L. Costa).

https://doi.org/10.1016/j.jhydrol.2023.129886
Received 24 January 2023; Received in revised form 19 June 2023; Accepted 25 June 2023
Available online 28 June 2023

Nomenclature

Symbols

GLP	N-phosphonomethylglycine, Glyphosate
AMPA	Aminomethylphosphonic-acid
KBr	Potassium bromide, Br^- bromide
ET	Evapotranspiration
ET_0	Reference ET
ET_c	Potential crop evapotranspiration
K_c	Crop coefficient (\)
Z_e	Depth of influence of the active roots transpiration (m)
P	Precipitation (mm/h or mm/d)
T	Temperature (°C)
θ	Volumetric Water Content (m^3/m^3)
K_f	Freundlich adsorption coefficient ($\mu g^{(1-1/\eta)}$ $mL^{1/\eta}$ g^{-1})
K_d	Angular coefficient of the linear relationships adopted in the simulations that describe the Freundlich soil-water partition model.

Acronym

SN_p	Settolo North plot
SS_p	Settolo South plot
CE_p	Colnù East plot
CW_p	Colnù West plot
DOCG	Denomination of Controlled and Guaranteed Origin
PPPs	Plant Protection Products
DPC	Dead Plant Coverage
BGL	Below Ground Level
BRTSim	Bio-Reactive Transport Simulator
PEST	Model-independent Parameter ESTimator and uncertainty analysis
SWAT	Sub-surface Water quality and Agricultural pracTices monitoring

that in the Treviso province a volume of 101.5 million cubic meters of water is extracted every year from wells to supply drinking water to a population of approximately 900,000 inhabitants (Trentin, 2021) and that about 60% of this volume is supplied from the Prosecco area. The GLP spread as a post-emergence herbicide suitable for a large variety of crops, has been supported worldwide since its introduction in 1974 due to its claimed effectiveness, biodegradability, and apparent low mobility (Baylis, 2000). However, thanks to the development of new quantification techniques (Pires Rosa, 2018), GLP has been identified in an increasing number of environmental monitoring programs. The results achieved in the analysis of GLP residues distribution in European agricultural soils (Silva et al., 2018) and a global-scale hazard analysis correlated to its persistence (Maggi et al., 2020), provided a worrying picture related to the consequences of its widespread use. Along with the long-standing dispute about its negative effects on human health (Székács and Darvas, 2018), limited information is available on its decay during the infiltration in the vadose zone and its ability to alter the quality of the groundwater eventually reaching a well supplying drinking water.

GLP and its principal degradation metabolite, aminomethylphosphonic-acid (AMPA), have been commonly detected in both surface and subsurface waters by field surveys (e.g., Battaglin et al., 2014). Studies at the catchment scale (10^1 km^2 to 10^2 km^2) on the distribution of the two chemicals residues, revealed strong correlation between observed rainfall events and the herbicide detection in surface waters (Peruzzo et al., 2008) and higher fractions of GLP and AMPA adsorbed to suspended particles and sediments when transported by water streams (Aparicio et al., 2013). This evidence has been broadly verified in other research works about the quality of water coming from agricultural plots (10^{-3} km^2 to 10^{-2} km^2) subjected to surface runoff. Todorovic et al. (2014) investigated the influence of heavy erosive precipitations falling "very shortly" after the application of the GLP. This allowed the authors to ascertain the main effects of soil structure and preferential flows on the dissipation of the herbicide and AMPA. Similarly, Napoli et al. (2016) observed that rainfall, occurring within a month after the treatment of a vineyard, causes the transport of high fractions of both species. At the regional scale, Poiger et al. (2017) measured the herbicide concentration in more than 1000 samples collected from groundwater, streams, lakes, and wastewater treatment plants effluents in the province of Zurich. GLP was mainly detected at elevated concentrations in surface waters while fewer occurrences of the herbicide were observed in groundwater. The particle-facilitated transport, i.e., the movement of soil particles with adsorbed chemical species (Okada et al., 2014), as principal mechanism for the GLP movement was verified in soil-flume laboratory experiments developed by Yang et al. (2015) and Bento et al. (2018). The former confirmed the risks for GLP offsite transport caused by early rainfalls after its application, while the latter linked the particle-bound transport to the content of organic-matter and to the fraction of clay minerals, both easily and rapidly transported with runoff. Tang et al. (2019) found similar evidence by developing a series of microcosm experiments on soil samples characterized by a different GLP exposure history. Also in this case, the adsorption of GLP to suspended mineral particles was observed in samples with higher fractions of silt and clay. The study included a modeling analysis of the various factors affecting the herbicide biodegradation, carried out applying the numerical model BRTSim (Maggi, 2019). Laboratory evidence on GLP biodegradation along with field data of precipitation and water table dynamics were implemented in the research work of la Cecilia et al. (2018) developed using the same model. The study numerically assessed the biodegradation and the infiltration of GLP and AMPA in a vineyard and in a wheat field located in the Po river Valley, Italy. GLP and bromide infiltration experiments were conducted by Okada et al. (2014, 2016) in controlled laboratory conditions using undisturbed soil columns collected in agricultural fields located in the Cordoba and Buenos Aires provinces, Argentina. The strong retention of glyphosate to the soil matrix was the dominant factor affecting glyphosate mobility in the soil profile. In both studies the authors stress that their results may underestimate the GLP leaching that could occur in the field via particle-facilitated transport under rainwater conditions.

It is manifest that a broad list of studies has been developed to evaluate the presence of GLP in ecosystems or its offsite transport by runoff after erosive precipitation events, while less attention was devoted to the subsurface environment where GLP evolution is affected by physical infiltration processes dominated by heterogeneity of the formations and preferential transport pathways at the field scale (e.g., Kjær et al. 2011, Mencaroni et al. 2023).

Building on a previous experimental study (Mencaroni et al., 2022), whereby the possible interactions between the PPPs and wellhead protection areas were investigated in two field sites located in the province of Treviso (Italy), the aim of this paper is to acquire, through numerical modeling, a better understanding of the mechanisms governing the evolution of the GLP transport / migration / leaching process through the unsaturated soil, from the treated soil to the water table, and the related arrival times. Since 2019, glyphosate is banned in the DOCG area of the Prosecco production, but it remains currently approved for use in the EU until 15 December 2023 (Commission Implementing Regulation (EU) 2022/2364). For this reason, the importance of a correct and thorough evaluation of its possible interactions with the groundwater resource remains. Following up on the experimental campaign, the field data collected at different depths and subjected to natural forcing, are here analyzed with a physically based model accounting for the soil

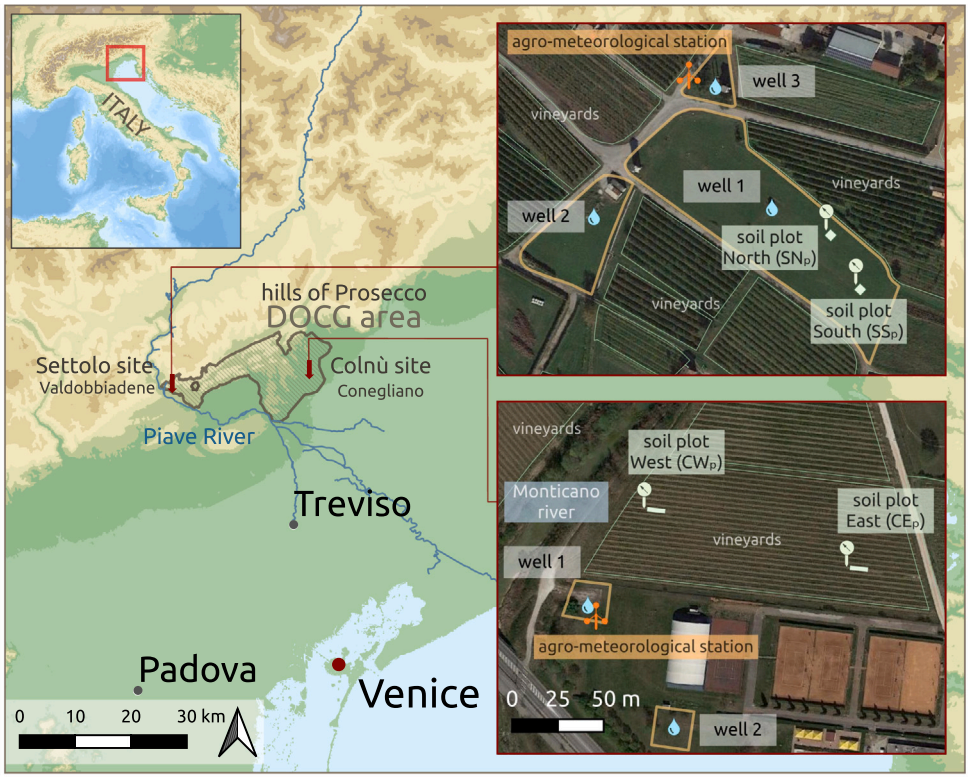

Fig. 1. The DOCG area of the Prosecco wine production and the maps of the two experimental sites: Settolo at Valdobbiadene and Colnù at Conegliano. The red arrows indicate the location of the two sites within the Veneto region and the DOCG production area of Prosecco (delimited area). In the maps of the two sites, the yellow framed areas are owned by the two water utility companies, Alto Trevigiano Servizi at Settolo and Piave Servizi at Colnù. (For interpretation of the references to color in this figure legend, the reader is referred to the web version of this article.)

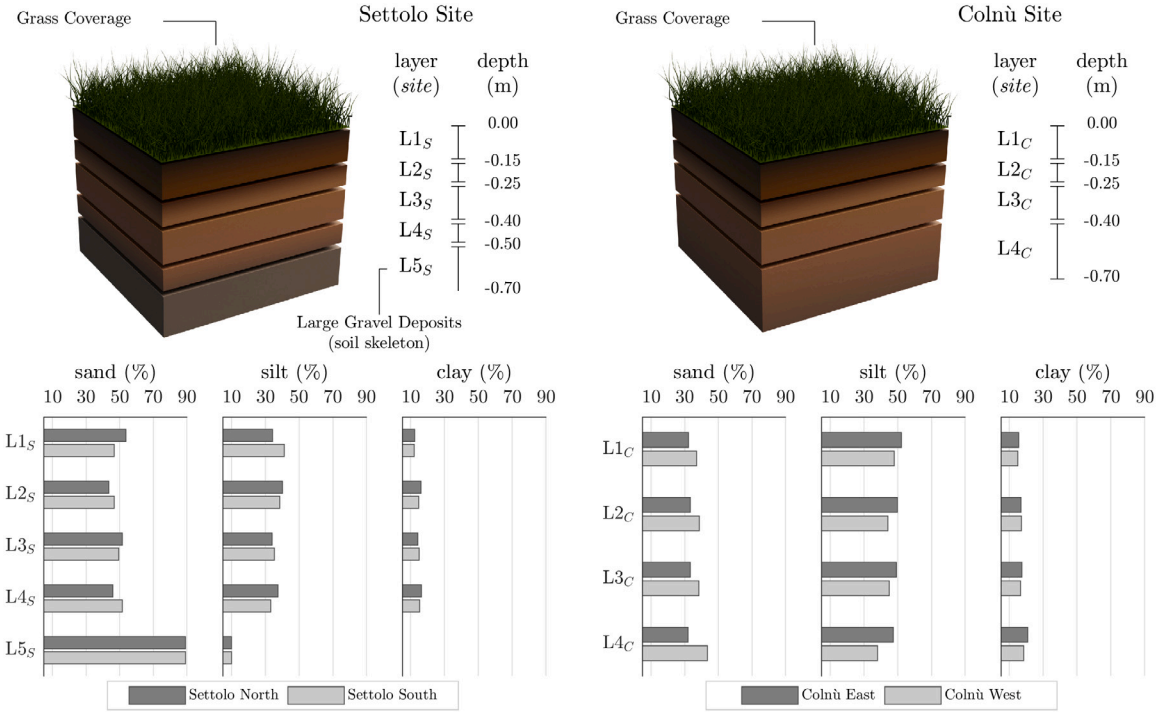

Fig. 2. Soil textures observed in the two soil-plots of the Settolo and Colnù experimental sites.

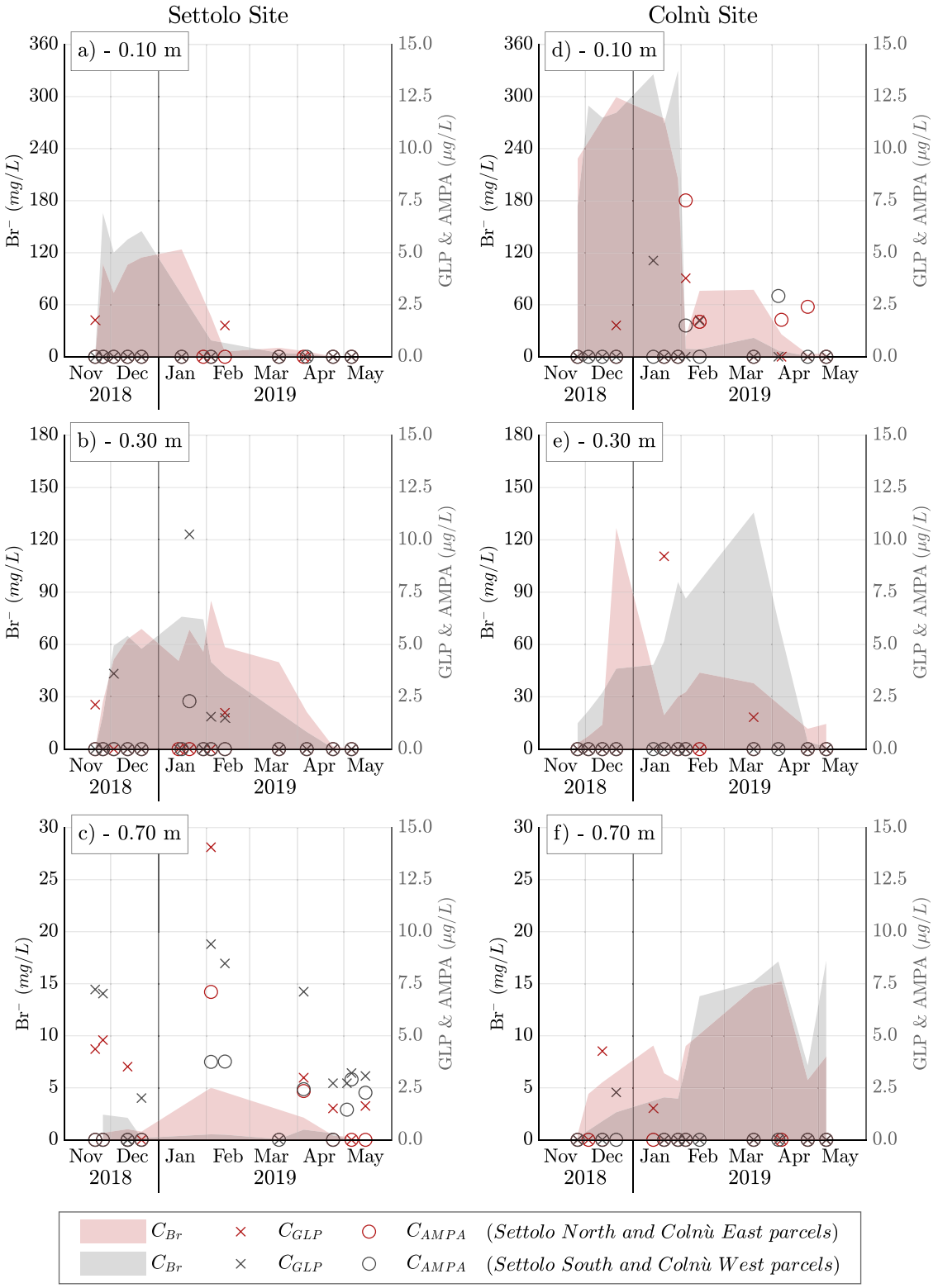

Fig. 3. Time evolution of bromide (Br^-), GLP, and AMPA as measured in the two experimental sites. (Data values from Mencaroni et al., 2022). Data from the Settolo site are reported on the left column while the ones from the Colnù site are reported on the right column. The time variation of the bromide concentration is represented as colored areas (gray and pink to distinguish the two plots of each experimental site) and refer to the left vertical axes. Glyphosate and AMPA are indicated by the cross and circle symbols, respectively. (For interpretation of the references to color in this figure legend, the reader is referred to the web version of this article.)

hydraulic properties and physical–chemical processes taking place in the vadose zone. To the best of our knowledge, a physics-based model of herbicide transport through different depths of the unsaturated zone is developed for the first time based on field experiments rather than on data deduced from laboratory soil columns.

2. Material and methods

2.1. Experimental sites

Two areas located in the Province of Treviso (Italy), Settolo - Valdobbiadene and Colnù - Conegliano, were considered (Fig. 1). They host two systems of wells supplying water for human consumption, surrounded by vineyards of Glera, the grape variety for Prosecco production, cultivated on different soils and hydrological conditions. To study the evolution and the transport of pesticides subjected to the natural forcing, two experimental sites were set up in October 2018. They consisted of an agrometeorological station (DeltaOHM, Italy) and two subsurface monitoring systems composed of multi-sensors probes (HD3910.1, DeltaOHM, Italy), pore water samplers (SPE20, UMS, Germany) and pan lysimeters (Supplementary Material, Figure A.1). The agrometeorological stations were equipped with standard sensors suitable for the measurement of rainfall (mm), temperature (°C), atmospheric pressure (mbar), relative humidity (%), wind direction (°) and velocity (m/s), and solar radiation (W/m^2). The measure interval is 10 minutes. Multi-parametric sensors, to gauge hourly soil temperature T (°C) and volumetric water content θ (m^3/m^3), and pore water samplers were installed at three depths, 0.10 m, 0.30 m, and 0.70 m along the vertical. At Settolo, due to the presence of large gravel deposits starting from a depth of 0.50 m, it was not possible to install the pore water sampler at −0.70 m, which was instead replaced with a pan lysimeter. Before installation the soil moisture sensors, operating with frequency domain reflectometry technology, were calibrated in the laboratory of the Department of Agronomy, Food, Natural resources, Animals and Environment (DAFNAE – University of Padova) according to the thermogravimetric method (Starr and Paltineanu, 2002), achieving an accuracy of ±3% on soil samples taken in triplicate for each experimental site. The soil monitoring equipment was installed in two 25 m^2 plots per site named Settolo North plot (SN_p) and Settolo South plot (SS_p) for the Settolo site and Colnù East plot (CE_p) and Colnù West plot (CW_p) for the Colnù site. The two plots were positioned at reciprocal distances of 30 m and 115 m within the Settolo and the Colnù sites, respectively. At the Settolo site, the soil plots were located inside the uncultivated area around the well 1 (Fig. 1). At the Colnù site, the two soil plots were located between the grapevine rows of the vineyard located North to both the pumping wells.

2.2. Sampling and data collection

The experimental activities are presented in detail in Mencaroni et al. (2022). Here, we report a brief summary of the relevant elements for the modeling activities. In August 2018, a preliminary sampling campaign was performed at the site plots to obtain information on the soil physical and chemical properties (Suppl. Mat., Section B, Table B.1). The soil texture and bulk density variation with depth, and the glyphosate adsorption capacity of the soil, were measured on disturbed core samples. Four core samples were collected just outside the site plots (down to −0.70 m at Colnù and down to −0.50 m at Settolo due to the aforementioned presence of gravel deposit) to prevent preferential infiltration pathways within the areas selected for the subsequent monitoring activity. In November 2018, the applications of a tracer and an herbicide, commonly involved in the protection of the vineyards from weeds and other unwanted plant species, were performed on the four site plots. The tracer, potassium bromide (KBr), was applied on a 7.5 m^2 area in the center of each site plot, while the pesticide was applied on the whole plot area. The pesticide applied on the four plots was the commercial herbicide Chikara Duo containing glyphosate (GLP — 28.8%) and flazasulfuron. Its application was carried out simulating the pesticide spreading mechanism of a boom sprayer through a manually conducted tool equipped with an air-actuated nozzle spray bar. For both Chikara and potassium bromide, a spatially uniform step-injection (about 10 seconds) was developed. The concentrations used for the application on the four site plots are listed in Table 1. The water samples were collected after each rainfall event by connecting a vacuum pump (Vacuum Porter, Meter Group) to the porous cups and the pan lysimeters, and by applying a −0.55 bar negative pressure. They were stored in plastic bottles (Nalgene) to avoid any adsorption of the investigated chemicals. The presence of GLP and AMPA was recognized in terms of concentration and mass fraction by analyzing the water samples and the soil samples through a specifically developed method based on UHPLC–ESI-MS/MS after derivatization (Carretta et al., 2019). The limits of detection (LOD) and quantification (LOQ) were established to be 0.20 and 0.50 μg/L, respectively, for glyphosate and 0.05 and 0.10 μg/L respectively for AMPA. Adsorption analyses were developed on three sections of each core sample (0.00 to −0.15 m, −0.15 m to −0.40 m, −0.40 m to −0.70 m) to quantify the fraction of GLP adsorbed to the soil particles (Mencaroni et al., 2022). From the laboratory adsorption analyses developed on soil samples, the value of the Freundlich partition coefficient K_f was obtained via simple interpolation of the well-known relationship

$$Q_e = K_f * C_e^{(1/\eta)} \quad (1)$$

where Q_e is the amount of GLP adsorbed to soil particles (μg/g), C_e is the GLP concentration in water (μg/mL) and η is the regression constant.

We stress the fact that inside each plot the monitoring and sampling positions are aligned along one vertical, the study of the three-dimensional physical and chemical heterogeneity being out of scope of the research developed by Mencaroni et al. (2022).

Table 1
Concentrations and loads adopted for herbicide (he) on a 25 m^2 area and for the application of the tracer (tr) on a 7.5 m^2 area. C_{he} is the herbicide concentration, L_{he} is the herbicide load, C_{tr} is the tracer concentration, L_{tr} is the tracer load.

Index	Site plots				Unit
	Settolo		Colnù		
	North	South	East	West	
C_{he}	17.14	17.14	17.14	17.14	g/L
L_{he}	0.16	0.16	0.18	0.24	g/m^2
C_{tr}	112.72	112.08	106.91	106.91	g/L
L_{tr}	10.37	10.76	10.26	9.55	g/m^2

2.3. Numerical modeling

According to the available data, the numerical analysis has been developed using a one-dimensional model to simulate the water infiltration, the tracer evolution, and the glyphosate evolution processes down to a depth of 0.70 m below ground level (BGL). The BRTSim code (Bioreactive Transport Simulator) developed by Maggi (2019) was adopted for its capability to handle the network of kinetic reactions and physical processes characterizing the root zone and affecting the GLP evolution by biodegradation, transport, and sorption–desorption dynamics (la Cecilia et al., 2018). BRTSim is a finite-volume computational solver for biogeochemical reaction–advection–diffusion processes in porous and non-porous media. It is suitable to describe water flow in soils, to track transport of aqueous chemicals and to assess their chemical equilibrium and their decomposition rates in both chemical and biochemical reactions. BRTSim solves a multi-phase flow problem over a defined domain considering the solid (S), liquid (L), and gas (G) phases. A fourth independent phase (the biological phase B) is also accounted for given its interactions with L and G phases.

Table 2
Stylized simulation scenarios.

Scenario	Limit value of the volumetric water content φ' [\]		Calibration						Validation	Tracer simulation	GLP simulation
	Settolo	Colnù	Calibration time period t_{cal} [d]	Depth of active roots Z_e [m]	Crop coefficient K_c [\]	Parameters			Validation time period t_{val} [d]		
						Permeability	Van Genuchten coefficients				
						k [m^2]	α [1/Pa]	n [\]			
0	Estimated with the ROSETTA code		No	0.30	0.3–0.9 (time varying)	Estimated with the ROSETTA code			93	None	None
1	Derived from Bulk density	θ_{max}	156	0.30	0.3–0.9 (time varying)	Calibrated	Measured by lab analysis		93	None	None
2	Bulk density	θ_{max}	156	0.30	0.3–0.9 (time varying)	Calibrated	Calibrated	Calibrated	93	YES	None
3	Bulk density	θ_{max}	156	0.00–0.30 (time varying)	0.3–0.9 (time varying)	Calibrated	Calibrated	Calibrated	93	YES	YES

θ_{max}: maximum volumetric water content measured on-site.

Table 3
Flowrate values (Q) and concentrations (M) used in the simulation of the Bromide application.

Index	Site plots (application area A = 7.5 m^2)				Unit
	Settolo		Colnù		
	North	South	East	West	
Q_{Br}	0.069	0.072	0.072	0.067	l/s
M_{Br}	1.411	1.403	1.338	1.338	mol/L

Table 4
Values and log-values of the linear adsorption coefficient K_d ($\mu g\ g^{-1}$ mL μg^{-1}) used in the GLP evolution modeling.
Source: Data from Mencaroni et al. (2022).

	SN_p	SS_p	CE_p	CW_p
K_d	100.0	109.6	707.9	346.7
$Log_{10}K_d$	2.00	2.04	2.85	2.54

The soil moisture dynamics are dealt with a finite volume scheme solving the one-dimensional formulation of the Richards' equation (Richards, 1931) along the vertical, considering also sink terms. By the latter, it is possible to account for the solutes uptake process carried out by the plants along the roots depth. On the other hand, no hysteresis in the wetting/drying curves and no factor of water uptake reduction for low water contents are considered.

In the code, the evolution of chemical species (GLP and Br^- in the developed model) is addressed by solving the following mass conservation law for the mass M_β^j of species j in phases β = L,G in a volume V of the solving domain,

$$\frac{\partial M_\beta^j}{\partial t} = \int_\Gamma \rho_{\beta e}\left(v_\beta X_\beta^j - D_\beta^j \nabla_z X_\beta^j\right) d\Gamma + \int_V \rho_{\beta e} u_\beta X_\beta^j dV \pm \int_V r_\beta^j \rho_{\beta e} dV \quad (2)$$

where $\rho_{\beta e}$ is the effective phase density (accounting for the effect of dissolved species), v_β corresponds to the Darcy's velocity of phase β through the surface Γ of a volume toward an adjacent volume, X_β^j and D_β^j are the mass fraction and diffusivity of species j in β, respectively, u_β is the sink term of phase β, and r_β is the rate of production or destruction of species j, resulting from both kinetic and equilibrium reactions. BRTSim does not handle hydrodynamic dispersion, but the available data did not allow to identify the effects related to this phenomenon. Therefore, instead of use a dispersion coefficient as a lumped coefficient including all the uncertainties of the evolution processes, we decided to analyze the experimental evidences via an advection–reaction–diffusion model, discussing in a second step eventual mismatches between the former and the numerical results.

2.3.1. Model set-up

For each site position, the model domain represented the experimental plot vertically subdivided in seventeen elements of thicknesses Δ_i and volumes $\Delta_i * A_t$, where A_t = 25 m^2 when modeling glyphosate and A_t = 7.5 m^2 for the tracer. Although the model was one-dimensional, the area of the treated surfaces was used for the computation of the surficial-incoming volume fluxes of rainwater, potassium bromide, and glyphosate, all expressed in m^3/s. For each element, the following features must be defined: (i) depth, volume, interface areas with the adjacent elements, and distance between above and below centers of mass (nodes); (ii) soil texture and hydraulic properties (permeability k, van Genuchten retention curve coefficients α and n, and residual liquid and gas saturation values); (iii) initial conditions of soil saturation, soil temperature and gas pressure. The thickness of the topmost element has been set equal to 0.025 m, while for the other elements it has been set equal to 0.05 m, in order to obtain an exact correspondence between the third, seventh, and fifteenth elements central nodes and the capacitive sensors and water pore samplers installed at depths of 0.10 m, 0.30 m and 0.70 m, respectively.

Neumann's (second type) boundary conditions (BCs) for the water infiltration process were set at the surface and at the bottom of the domain, with fluxes equal to the hydrological forcing (rainfall and evapotranspiration) on the surface, and zero at the bottom. A free water drainage condition at the depth of 0.70 m BGL was approximated by assigning a very large volume (5×10^6 m^3) to the seventeenth element (BRTSim v3.1a User Manual, Maggi 2019).

Arbitrary initial conditions (ICs) for soil moisture and soil-water temperature have been imposed at the beginning of a spin-up period of 90 days, during which the first 30 days of hydrological forcing were repeated for three times to minimize the influence of the initial values on the model results. Specifically, the soil saturation was set equal to 98% for the elements from Δ_{01} to Δ_{15} and 60% for the elements Δ_{16} and Δ_{17}, while the soil-water temperature was considered constant along the vertical direction and equal to the daily mean temperature of the first day of the simulated period and the gas pressure was set equal to the daily averaged atmospheric pressure gauged by the meteorological station in the first day of the simulated period.

Evaporation and root water uptake were modeled as outward liquid fluxes along the depth Z_e (Section 2.3.3), which value was differently assumed across the simulated scenarios, as described in Section 2.3.4. Despite the position of the Colnù plots (Section 2.1), grass and grass

root system were assumed for all the plots, the grapevine root system being far from the capacitive sensors and the pore-water samplers positions in both the experimental sites.

Glyphosate degradation was simulated using the kinetic network developed by la Cecilia and Maggi (2018), including the GLP degradation to its principal metabolite AMPA (see 3.5) and accounting for the growth and decay of the involved microbial functional groups (GLP biodegraders). Initial and boundary conditions for the GLP biodegraders concentration, the substrates concentration for kinetic biological reactions, the reagents concentration for chemical equilibrium reaction, the dissolved oxygen concentration [O_2], and the pH value (H^+ concentration, [H^+]), were set according to la Cecilia et al. (2018). IC for [O_2] was set depending on the depth, with [O_2] = 1e−4 mol/L (3.20 mg/L) up to the depth of 0.70 m BGL, and [O_2] = 1e−5 (0.32 mg/L) below the depth of 0.70 m. IC for [H^+] was set constant along the model domain, [H+] = 1e−7 mol/L (pH = 7). Neumann's BCs were set for the two chemical species, assuming the same concentrations set in the topmost element ([O2] = 1e−4 mol/L, [H+] = 1e−7 mol/L) for the liquid fluxes incoming from the ground surface (rainfall forcing), while no-flux condition was set at the bottom.

As for the transport of the reactive solutes in the soil, only the GLP transport was simulated (see 3.5), the adsorption coefficients deduced from laboratory analyses being available for the GLP only and not for the herbicide degradation metabolites (Mencaroni et al., 2022). An average value for the diffusion coefficient in the liquid phase was set $D_s = 1e^{-9}$ m^2/s for both Br^- and GLP. Gas flow entering the model domain and advection–diffusion of chemical species in the gas phase were not considered.

2.3.2. Model calibration and validation

Water content observations collected at depths of 0.10 m, 0.30 m and 0.70 m were used to calibrate/validate the infiltration model, while bromide and GLP concentration data were only used to test the predictive capabilities of the coupled infiltration–advection/reaction model. The hydraulic parameters, namely soil porosity φ, permeability k and retention curve coefficients - α and n (van Genuchten, 1980), were initially estimated from soil-textures data using the ROSETTA code (Schaap et al., 2001) and then were calibrated with PEST (Doherty and Hunt, 2010) by minimizing the sum of squared differences between modeled and observed θ values. The Kling-Gupta efficiency index (KGE) (Gupta et al., 2009) was also computed, as an additional goodness of fit metric of the simulations, even if it was not the objective function of the calibration. The KGE index is defined as follows:

$$KGE = 1 - \sqrt{(r-1)^2 + (\alpha-1)^2 + (\beta-1)^2} \quad (3)$$

with

$$\alpha = \sigma_s/\sigma_o$$

and

$$\beta = \mu_s/\mu_o$$

r being the correlation coefficient between simulated and observed values ($r \leq 1$, where unity represents the optimal value), α the ratio between the standard deviations of simulated and observed values, β the ratio between the mean simulated and mean observed. In the assessment of the model efficiency, KGE gives more weight to similar behaviors between observed and modeled trends compared to the standard sum of squared errors (see Gupta et al., 2009). This peculiarity makes this metric more suitable for hydrological models where the physical quantities are often characterized, as in this case, by peaks and high variability.

2.3.3. Hydrological forcing

The input hydrological forcing, considered as the main driving mechanism for rainwater and solutes infiltration, was based on the rainfall depths acquired by the rain gauges and the variables observed by the two agro-meteorological stations, since no irrigation was applied on the soil plots during the simulated period. The potential evapotranspiration (ET) was computed using the single crop coefficient approach $ET_c = K_c \times ET_0$ provided by Allen et al. (1998), the reference evapotranspiration (ET_0) being assessed using the Penman–Monteith equation. The crop coefficient K_c [\], defined as the ratio of the crop ET_c and the reference ET_0, was assumed constant or variable in time depending on the vitality of the vegetation cover and the glyphosate herbicide effects (dead plant coverage — DPC). The depth of influence of the active-roots transpiration, Z_e [m], was assumed constant or variable according to the vegetation cover (grass) of the four experimental soil-plots. Therefore, to simulate the vegetation decay due to the herbicide application, the depth Z_e was set following the time behavior of K_c (Allen et al., 1998).

2.3.4. Simulated scenarios

The simulation scenarios reported in Table 2 were modeled by varying the depth of influence of the active-roots transpiration, Z_e, the crop coefficient, K_c, the permeability, k, the van Genuchten - water retention curve model coefficients, α and n, to test the influence of each parameter on the infiltration process, also using water retention curves deduced from laboratory analyses (Suppl. Mat., Section C, Figures C.1 and C.2). Table 2 shows the parameters adopted in the four site-plots to distinguish the simulated scenarios. The values adopted for Z_e and K_c, equally set in the four soil-plots, are also reported. Detailed values of the plot-specific hydraulic parameters, k, α and n, can be found in Table D.1 (Suppl. Mat., Section D), subdivided by soil-layer and simulated scenario.

The numerical code also required the definition of the maximum volumetric water content that can be reached under the forcing conditions. Theoretically, this value corresponds to the porosity φ, but during the infiltration process that takes place in field conditions, air bubbles entrapped in the soil matrix can play an important role, reducing the maximum volumetric water content to a value $\varphi' \leq \varphi$. In a first approximation (Scenario 0) φ' was set equal to φ, the latter being derived from the soil texture data by means of the ROSETTA code (Schaap et al., 2001). In the other scenarios (s1, s2, and s3), a more appropriate φ' value was estimated based on the maximum volumetric water content values measured in the field or on the bulk densities when the former gave nonphysical values. The values of φ and φ' related to the soil layers of the site plots are available in the aforementioned Table B.1 (Suppl. Mat., Section B).

All the scenarios simulated the rainwater infiltration process, while the tracer and the glyphosate transport processes were only considered in the scenarios performing better in terms of water infiltration (Scenarios 2 and 3). In the following, we briefly describe the simulations by focusing mainly on the variations introduced with each scenario.

Scenario 0. The water infiltration process was simulated implementing the soil hydraulic parameters k, α, and n obtained through the ROSETTA code (Suppl. Mat., Table B.1 and Table D.1). Z_e and K_c were set constant and time varying respectively, according to Allen et al. (1998). Z_e was set equal to 0.30 m to simulate the transpiration carried out by the root apparatus of the grass cover. Thus, the ET_c water flux was simulated as a water withdrawal proportionally distributed along a depth of 0.30 m. K_c was assumed equal to 0.9 until the pesticide application and equal to 0.3 for the next three months (Allen et al., 1998, Chapter 11).

Scenario 1. The retention curve coefficients α and n were derived by fitting the experimental water-retention curves obtained from the soil samples collected in the field (Section 2.2). The remaining hydraulic

paramenter, the permeability k obtained through the ROSETTA code, was calibrated along a 156-day period.

Scenario 2. The soil hydraulic parameters k, α, and n, previously obtained thorough the ROSETTA code, were calibrated along a 156-day period. The potassium bromide application was modeled as a 10 seconds step-injection, according to the experiments developed in the field (Section 2.2). Table 3 reports the fluxes and the molar concentrations of the injected solution implemented in the transport model for each site-plot. The flow-rate values were estimated based on the volume of the applied solution divided by the time of application (10 seconds), while the concentration values are the ones used in the field experiments.

Scenario 3. To account for the pesticide effects on the plant roots, the simulations were carried out assuming a dead plant coverage (DPC) period of six months (K_c = 0.3) since the site plot treatment. In the period in which K_c = 0.3, Z_e was reduced from 0.30 m to 0.00 m, the root water uptake being limited to the surface during the DPC period (Suppl. Mat., Section E, Figure E.2). As for the Scenario 2, the soil hydraulic parameters were calibrated along a 156-day period.

3. Results

3.1. Weather data

The first two months of the study period were characterized by abundant precipitations (with peaks of more than 50 mm/day and 20 mm/day observed in late October and in the second half of November, respectively) while smaller rainfall depths were observed during the remaining part of the winter (See Figs. 4a and 5a in Section 3.4). In 2019, the more significant precipitation events occurred at both the experimental sites in spring and autumn, when the annual maximum percentages of rainy days (almost 50%) were recorded. Similar daily mean temperatures were recorded in the two sites, ranging from −1.4 °C to 29.9 °C at the Settolo site and from −3.5 °C to 28.8 °C at the Colnù site, the mean values along the entire period being 13.6 °C and 13.0 °C, respectively. The monthly and the total amounts of rainfall from October 2018 to September 2019 show that Settolo was affected by more rain although the number of rainy days was almost equal in the two sites, the cumulative rainfall depth being about 1.3 times the one observed at Colnù . The rainfall intensity was higher in Settolo than in Colnù, the number of observed occurrences of rainfall intensity exceeding 5 mm/h being higher in the former site.

3.2. Soil texture analysis

Fig. 2 shows the soil textures in the two experimental sites and the differences observed in terms of sand, silt, and clay percentages (Suppl. Mat., Table B.1). Overall, the soil in Settolo is sandier than in Colnù, where silt is prevalent. Slight differences were also observed within the same experimental site, especially for the two shallower $L1_S$ soil layers of the Settolo site plots and the two deeper $L4_C$ soil layers of the Colnù site plots. The soil sampling in the former site was limited to the shallowest 50 cm due to the presence of coarse material. The texture of the Settolo $L5_S$ layers was derived from previous surveys (Crestani et al., 2015), and set equal to 89% sand, 10% silt and 1% clay.

3.3. Bromide and glyphosate concentrations

Fig. 3 shows the time evolution of the tracer, glyphosate, and AMPA, as measured in the two experimental sites (for further details, see Mencaroni et al., 2022). At −0.10 m (Fig. 3a and d) the concentrations of tracer in both the experimental sites remained high during the first three months (November 2018 to January 2019) due to the lack of significant rainfall events until the beginning of February 2019, when a sudden drop is manifest. At −0.30 m (Fig. 3b and e) a similar behavior was observed only at Colnù East, while in the West site the maximum concentration peak occurred in the second half of March 2019. At −0.70 m (Fig. 3c and f), the tracer concentrations are very low compared to shallower soil layers, with a dramatic reduction of the tracer mass and peaks shifted toward the second half of the sampling period. This indicates that the bromide mass was partially maintained along the vertical direction until a depth of 0.30 m, and then strongly reduced in deeper soil layers, likely due to losses through lateral paths.

The vertical dynamics of the herbicide seems to be strongly site-specific, with significant differences in concentration distribution and values between the experimental sites. This is probably due to both different soil features controlling the glyphosate decay and soil heterogeneity driving the solute along preferential paths different from the vertical one. In Settolo, glyphosate shows increasing concentrations from −0.10 to −0.70 m, while an opposite trend occurred in Colnù, where the herbicide concentrations gradually declined in passing from a depth of 0.10 m toward the deeper sampling points. After two months from the application, AMPA was found in both sites: at −0.10 m in the Colnù site and at −0.30 m in the Settolo site. Considering all the sampling depths, the maximum AMPA values measured in both sites were close to 7.5 μg/L, ranging for most of the samplings between concentrations of 1.5 μg/L and 4 μg/L.

3.4. Results of the numerical simulations

3.4.1. Infiltration processes

The simulated water content, obtained from the scenarios described in Section 2.3.4, are compared with observed data in Figs. 4–5, which also report the daily dynamics of rainfall and evapotranspiration. To improve the readability of the figures, one plot only for each site (SN_p for the Settolo site and CE_p for the Colnù site) is reported here, while the results for the remaining site plots can be found in the Supplementary Material (Section F, Figures F.1 and F.2). The graphs reported in the figures consider three depths (0.10 m, 0.30 m, and 0.70 m) and two groups of scenarios: (1) simulations developed using uncalibrated (Scenario 0) or calibrated hydraulic parameters (s2 and s3), and (2) simulations developed using laboratory-derived hydraulic parameters (Scenario 1). In Scenario 0, the hydraulic parameters were estimated by the ROSETTA code. Overall, the uncalibrated model simulated a dynamic similar to the observed soil water content, showing both peaks and tails comparable to the ones measured by the capacitive sensors. However, the experimental water content values were generally underestimated by the model, especially at −0.70 m in the SN_p plot, where the model predictions exhibit a negative shift of about 50% on the peaks while in dry periods the offset is even more than 50% (Fig. 5). Significant differences between simulated and observed θ values were found in SS_p and in CE_p site plots too, due to the lack of calibration. In Scenario 1, α and n were derived from the water retention curves obtained in the laboratory analysis, k was calibrated, and φ' was estimated based on the maximum volumetric water content values measured in the field or on the bulk densities, as specified in Section 2.3.4. This parameter configuration reduced the gap between modeled and observed θ values for all the plots (graphs c-2, d-2, e-2 of Figs. 4–5), showing the larger improvement at −0.70 m. However, observed θ values were still underestimated at −0.10 m at SN_p and along the entire depth at CE_p, showing differences up to 50% at the depth of 0.30 m. A possible explanation for this mismatch can be found in the laboratory-derived water retention curves (Suppl. Mat., Figure C.2) that showed an high uncertainty in the low values of the suction head (ψ < 1 m). By calibrating all the hydraulic parameters (Scenario 2) the simulation improved in the dry periods until March 2019 with shorter and better reproduced peaks. However, the water content observed in the period between the second half of March 2019 and the first half of April 2019 resulted again underestimated, highlighting a possible overestimation of the roots transpiration in the period after the herbicide application. This was partially corrected in Scenario 3 at all depths by assuming Z_e variable in time (Suppl. Mat.,

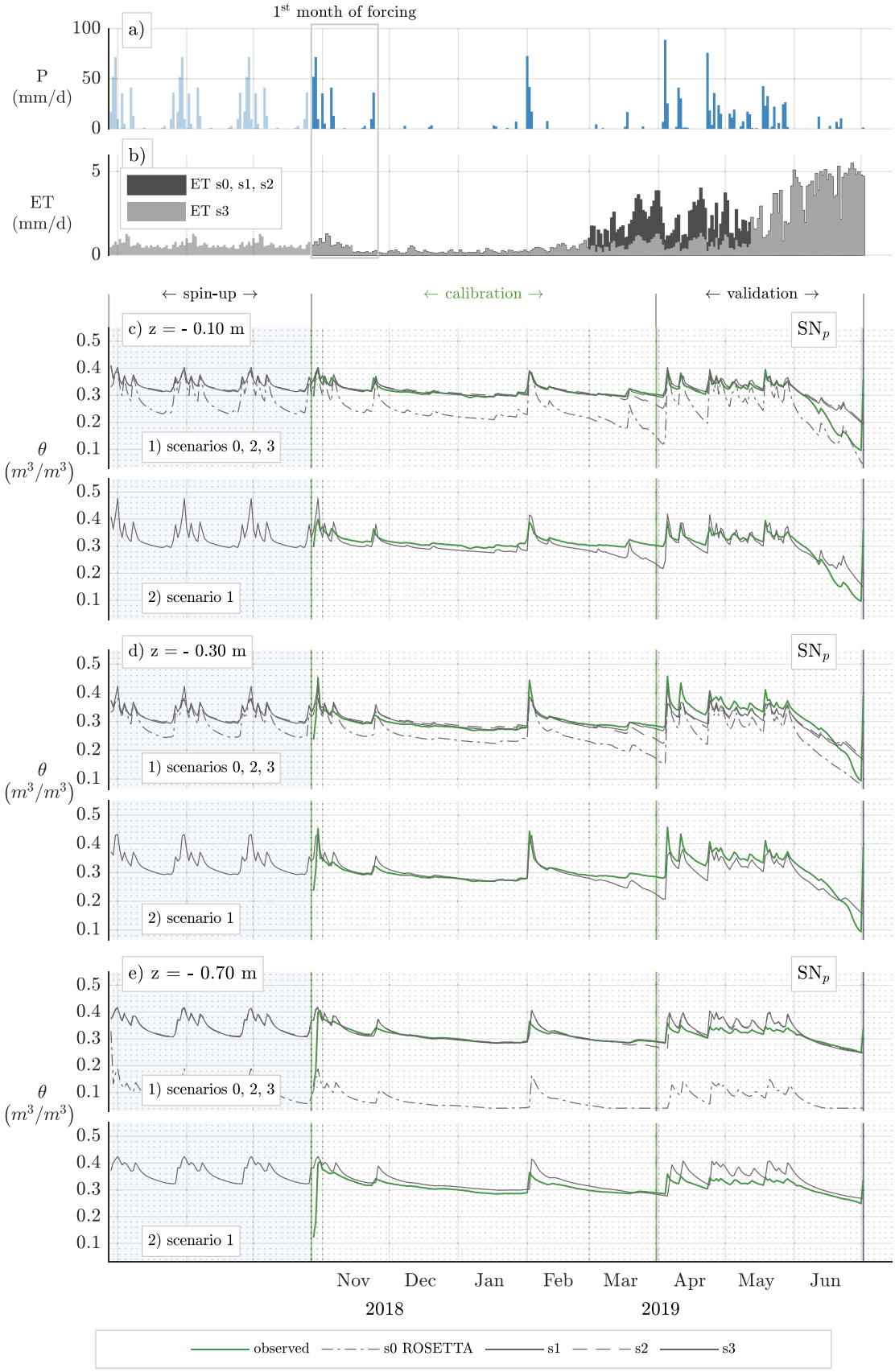

Fig. 4. Observed versus simulated water content (θ) at the experimental site-plot of Settolo North (SN_p), along with rainfall (P) and evapotranspiration (ET) forcing.

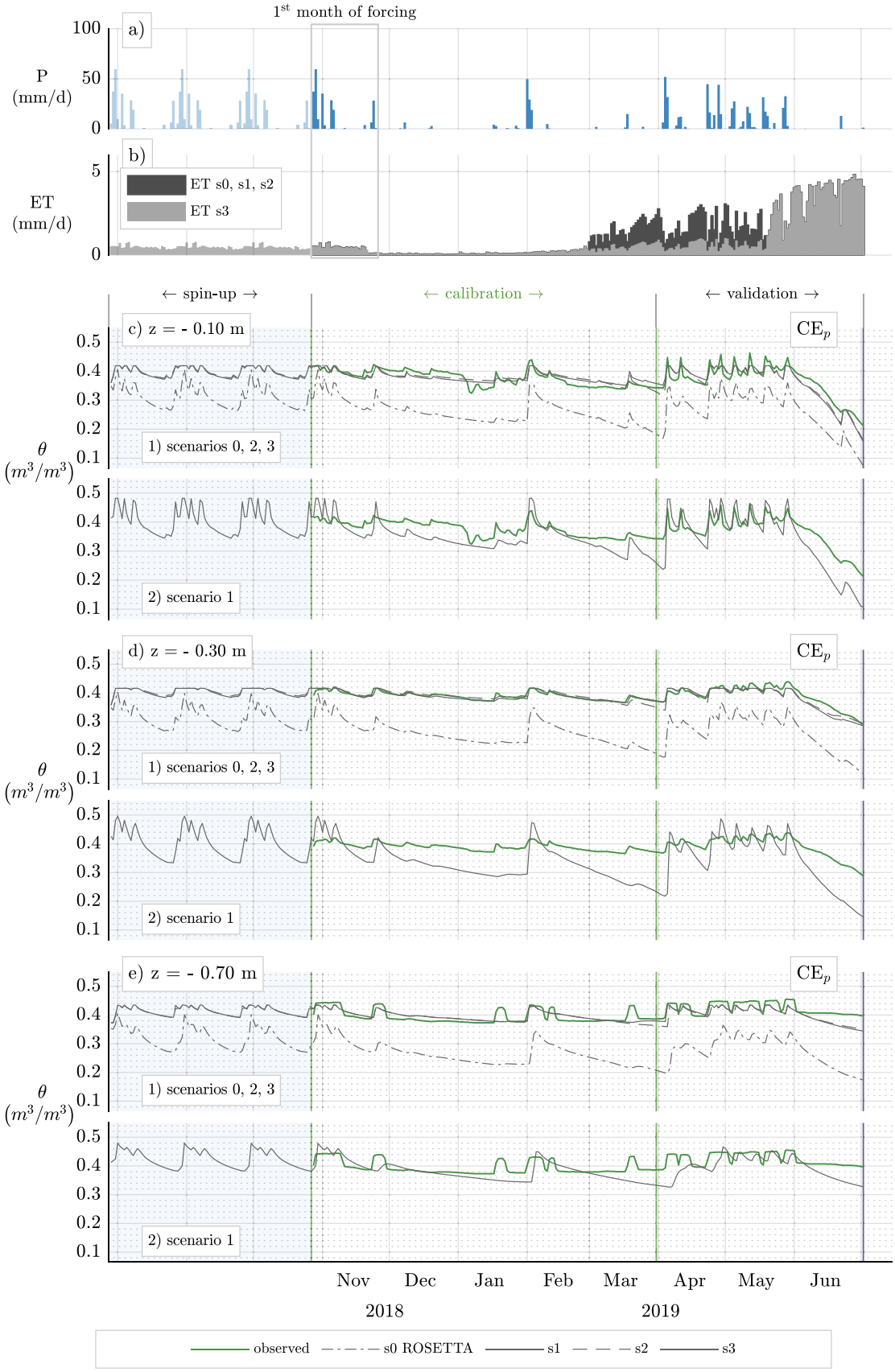

Fig. 5. Observed versus simulated water content (θ) at the experimental site-plot of Colnù East (CE_p), along with rainfall (P) and evapotranspiration (ET) forcing.

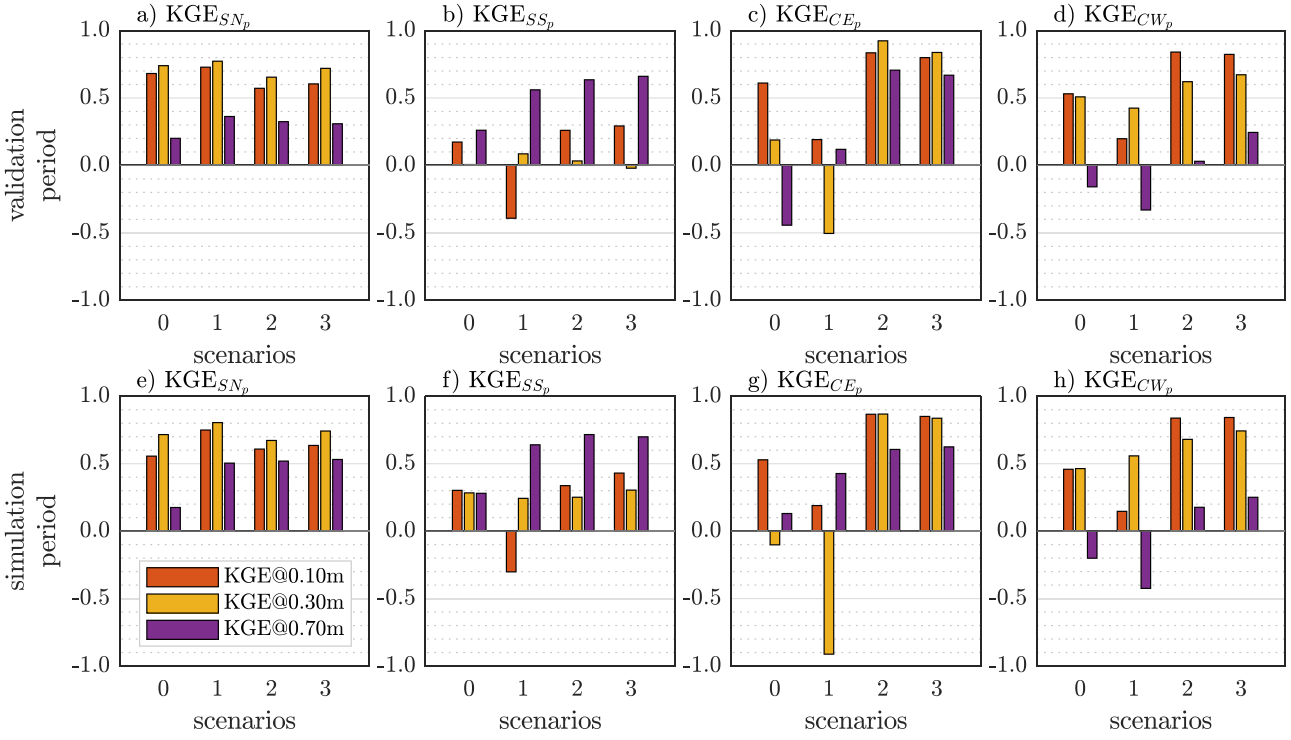

Fig. 6. Kling-Gupta efficiency indices (Gupta et al., 2009) for scenarios with calibrated (s2, s3) and laboratory data based (s1) parameters. Results for the scenario with uncalibrated ROSETTA-based parameters (s0) are also shown for comparison.

Figure E.2), which also generally improved the simulation at −0.70 m, even if the water content peaks in April and May 2019 resulted in slight overestimation. Overall, the calibration procedures developed in s2 and s3 involving all the hydraulic parameters initially estimated with the ROSETTA code, improved the capability of the model to simulate observed θ values.

To gain additional insights on the comparison of the simulated scenarios, the KGE indexes, computed by comparing the observed and the simulated θ values at the three depths (0.10 m, 0.30 m, and 0.70 m) of each site plot ($-\infty < \text{KGE} \leq 1$, where unity represents a perfect match), are reported in Fig. 6. In the figure the indexes related to the validation period (at the top) and the whole simulation period (calibration + validation, at the bottom) are presented. The goal is to better evaluate the model performances in the winter months after the herbicide application, and in the spring months, which are characterized by more frequent rainfall events. The calibration of the hydraulic parameters k, α, and n, in scenarios 2, and 3, improved the efficiency of the infiltration model in both the experimental sites. The best overall model performance was achieved for the Settolo North site-plot (Fig. 6a and e) along the entire depth, but good results were obtained also by the uncalibrated model (Scenario 0) at −0.10 m and at −0.30 m. A larger improvement compared to the uncalibrated scenario was achieved at the Colnù site (Fig. 6g and h), where the calibration of the hydraulic parameters as in Scenario 3 (K_c and Z_e variable in time) led to satisfactory results along the entire depth of both the site plots. In Scenario 1, the use of the coefficients α and n derived from the laboratory analysis (Suppl. Mat., Section C), led to a good modeling of the rainwater infiltration in the SN_p site-plot only. In SS_p, s1 gave the worse results, highlighting different performances depending on the site plot considered, even located only 30 m apart within the same experimental site. At the Colnù site, the use of the lab-derived α and n values (Scenario 1), led the model to poorly describe the rainwater infiltration process in both the site plots, with opposite results at −0.30 m and −0.70 m. While a good agreement between observed and modeled values is verified at −0.30 m at CW_p, the opposite occurs at the same depth at CE_p, and vice-versa at −0.70 m, confirming the aforementioned uncertainty in the low values of the suction head ($\psi <$ 1 m) used for α and n parameters estimation.

The best scenario is difficult to identify from Fig. 6. As an example, in CE_p the best scenario could be s2 (Fig. 6c) or s3 (Fig. 6g), while in SN_p the choice is between s1 and s3 (Fig. 6e). Scenarios 2 and 3 seem to be the best for both the two Colnù site plots (CE_p and CW_p), but for CW_p improvements in terms of KGE coefficient are not so evident compared to the other scenarios. Scenarios 2 and 3 did not show the best overall performances, but they are able to account for the transpiration activity of the plants' roots and they take advantage by the calibration of all the hydraulic parameters. Among the results achieved by using different sets of parameters, uncalibrated, calibrated, lab-derived, Scenarios 2 and 3 may be assumed as giving the best performances, from a global perspective. Moreover, the good results obtained in s3 supports the hypothesis that the effects of the herbicide on the transpiration activity of the plant's roots cannot be neglected at this scale.

3.4.2. Tracer evolution

The hydraulic parameters calibrated in Scenarios 2 and 3 were then used to simulate the bromide infiltration. Figs. 7 and 8 show the observed and simulated bromide concentration data in all the site plots, along with meteorological forcing (rainfall data and computed evapotranspiration). Overall, considering all the uncertainties related to field data and limitations of 1D modeling, the results are satisfactory. The timing of the tracer evolution was well reproduced by both simulation scenarios, with an underestimation of the tracer concentration only in the shallow layer (−0.10 m) of both the Colnù site plots and at −0.30 m in SS_p. The tracer application was simulated as a step injection (see Section 2.3.4), which is only an approximation of the real process. Probably due to this reason, observed and modeled concentrations show the maximum differences in the shallow layer of both the experimental sites. A very good agreement between simulated and observed concentrations was obtained at −0.30 m during the time-period spanning from the application (November 2018) to the beginning of February 2019 (Figs. 7e and 8e), except for SS_p where an abrupt

reduction of concentration was measured in the months just following the application. Similar discrepancies with the modeled results, i.e., an overestimation of the observed concentrations, are generally manifest at −0.70 m. This overestimation is more pronounced at Settolo, where the maximum concentrations observed at −0.70 m, 5.00 mg/L and 2.42 mg/L for SN_p and SS_p, respectively, are much lower than the corresponding values observed at the depth of 0.30 m, 85.12 mg/L and 75.92 mg/L respectively. Moreover, the SS_p values at −0.30 m are much lower than the ones observed at −0.10 m. Different hypotheses can explain this behavior. First, difficulties related to the soil-water sampling in the field could have affected the proper accounting of the Br^- concentration. Anyway, the strong heterogeneity observed in the Settolo site soil texture, just at −0.50 m BGL, suggests another possible explanation, that is a three dimensional structure of the soil could have caused lateral flow processes that could not be captured by the monitoring set-up. Last, the Br^- has probably been strongly affected by dilution between −0.30 m and −0.70 m, where it reached the pan lysimeter.

3.5. Glyphosate evolution

The GLP evolution was simulated with the hydraulic parameters calibrated in Scenario 3, the differences between tracer transport simulations in scenarios 3 and 2 being negligible. We adopted the site-specific GLP adsorption coefficients obtained by Mencaroni et al. (2022), whereas the kinetics for GLP degradation to AMPA were assumed according to the literature (la Cecilia and Maggi, 2018; la Cecilia et al., 2018), as specified in Section 2.3.1. The Freundlich soil-water partition models, experimentally deduced from the soil samples (Mencaroni et al., 2022), are described in the range of GLP concentration observed in the field by a linear relationship, whose angular coefficients are the adsorption coefficients K_d (one for each soil-plot as reported in Table 4 were used in the simulations). The K_d values show evident differences between the two sites, with the mean value in Colnù almost five times larger than in Settolo. A significant variability is also manifest between the two site plots in the Colnù site, K_d in CE_p being approximately twice the one in CW_p.

The comparisons between observed and simulated GLP concentration values at the Settolo site and at the Colnù site, are reported in Figs. 9 and 10 respectively. The observed and the simulated concentration peak values show the same order of magnitude in the upper soil layers at Colnù as well as in the deeper soil layers at Settolo, but the numerical simulation results seem unable to capture the observed spatio-temporal dynamics of the herbicide. The adopted transport model (equilibrium-solute reactive transport model) suggests a continuous herbicide evolution in time and along the vertical, with simulated concentration values always different from zero after the GLP application and decreasing along the vertical. On the contrary, most of the GLP concentrations measured in the field are below the limit of detection, or show unexpected spikes, mainly after the intense rainfall events. For instance, an increase of concentration along the vertical direction is observed in both the Settolo site plots between −0.30 m and −0.70 m during the period between November and December 2018 after an intense rainfall event. The GLP monitoring in the field was developed by water samplings driven by the occurrence of rainfall events. The potential limits affecting this episodic data forced the use of a model consistent with data driven by the capability of the porous cups to capture the dissolved GLP fraction in the site-plots.

However, as discussed in the literature (Norgaard et al., 2014; Kjær et al., 2011; Borggaard and Gimsing, 2008; Jarvis, 2007), the glyphosate transport can occur in solution, in suspension, or as a combination of the two mechanisms, depending on the texture of the media (unstructured or structured soil). The particle-facilitated transport that occurs in the latter mechanism, could not be acknowledged by using the porous cups, while the pan lysimeters at −0.70 m in Settolo allowed the collection of both the transported fractions. The discrepancies between measured and modeled glyphosate concentration values, can be explained based on (i) measurement limits related to the soil water sampling (porous cups in 10/12 of the total sampling positions) and (ii) the subsequent choice of the model, without description of the colloidal transport along preferential flow-paths. Therefore, a reasonable agreement was obtained only, as previously mentioned, in the unstructured first layer of soil of the Colnù site, and in the bottom layer of the Settolo site, where the water samples were collected by the pan lysimeters. Moreover, the presence of high fractions of GLP adsorbed to the soil matrix, highlighted by the laboratory analyses (Mencaroni et al., 2022), supports the hypothesis of a combined mechanism of transport. We argue that, during particularly intense rainfall events, GLP adsorbed to solid grains of limited size can move along possible preferential pathways caused by the soil heterogeneity (e.g., Borggaard and Gimsing, 2008). The ability of the pan lysimiters to account for both the GLP transport mechanisms, is also suggested by the comparison between the time evolution of GLP and bromide, at different depths, shown in Fig. 11. In SN_p, the GLP time-evolution is consistent with bromide only at the depth of 0.70 m, where the finest soil particles, washed out by the more intense precipitation events, were collected by the pan lysimeter sampling system. Similar considerations cannot be applied for the Colnù site, where the porous cups prevented the collection of colloidal particles at any depth, and the discrepancies with the one-dimensional model results may be ascribed to the soil heterogeneity and related three-dimensional preferential paths (Kjær et al., 2011). In the Settolo site, differences between the Br^- and GLP mechanisms of transport are manifest by comparing Figs. 7 and 9. Due to the combined effect of tracer dilution and the complex structure of soil texture below −0.50 m, the Br-concentration showed an abrupt reduction, while the GLP, adsorbed to the finest soil grains mobilized by heavy rainfall, reached the pan lysimiters, even if a limited dissolved fraction moved according to the tracer.

Overall, despite the timing of precipitation in relation to the herbicide application (Norgaard et al., 2014; Jarvis, 2007) might have played a relevant role in Settolo and Colnù site-plots, these results suggest that in the site-specific developed experiments, the herbicide as well as the tracer evolution is affected by three-dimensional heterogeneous characteristics of the soil (Borggaard and Gimsing, 2008; Jarvis, 2007). Therefore, an improvement in the GLP evolution modeling, e.g. using a 3D model, requires first a different and more complex approach in both the soil characterization and the experimental data collection, even at the small scale here considered.

4. Conclusions

In this work, the hydrological modeling of field experimental data collected in the period November 2018–May 2019 has been presented and discussed. The data are related to the infiltration process and the evolution of a non-reactive tracer, potassium bromide (Br^-), and a glyphosate(GLP)-based herbicide until a depth of 0.70 m in the unsaturated soil of two experimental sites located in the province of Treviso, Italy. The available data collected along the vertical led to the choice of a one-dimensional model, able to capture the advective–reactive–diffusion processes. The hydraulic parameters governing the process of infiltration, assumed as the main driving mechanism for the herbicide transport, were calibrated based on water content data (θ) collected in the field. The observed θ and Br^- concentration values were well reproduced by the calibrated model until a depth of 0.30 m. At deeper positions, discrepancies between observed and modeled values pointed out the limits of the one-dimensional modeling of the infiltration process, suggesting that the tracer dilution process combined with strong soil heterogeneity may play a relevant role. The heterogeneity of soil texture has also a great impact on reactive and sorbing chemical species.

The measured data show a scarce mobility of the GLP. The limited herbicide concentrations were recognized in circumstances that are in

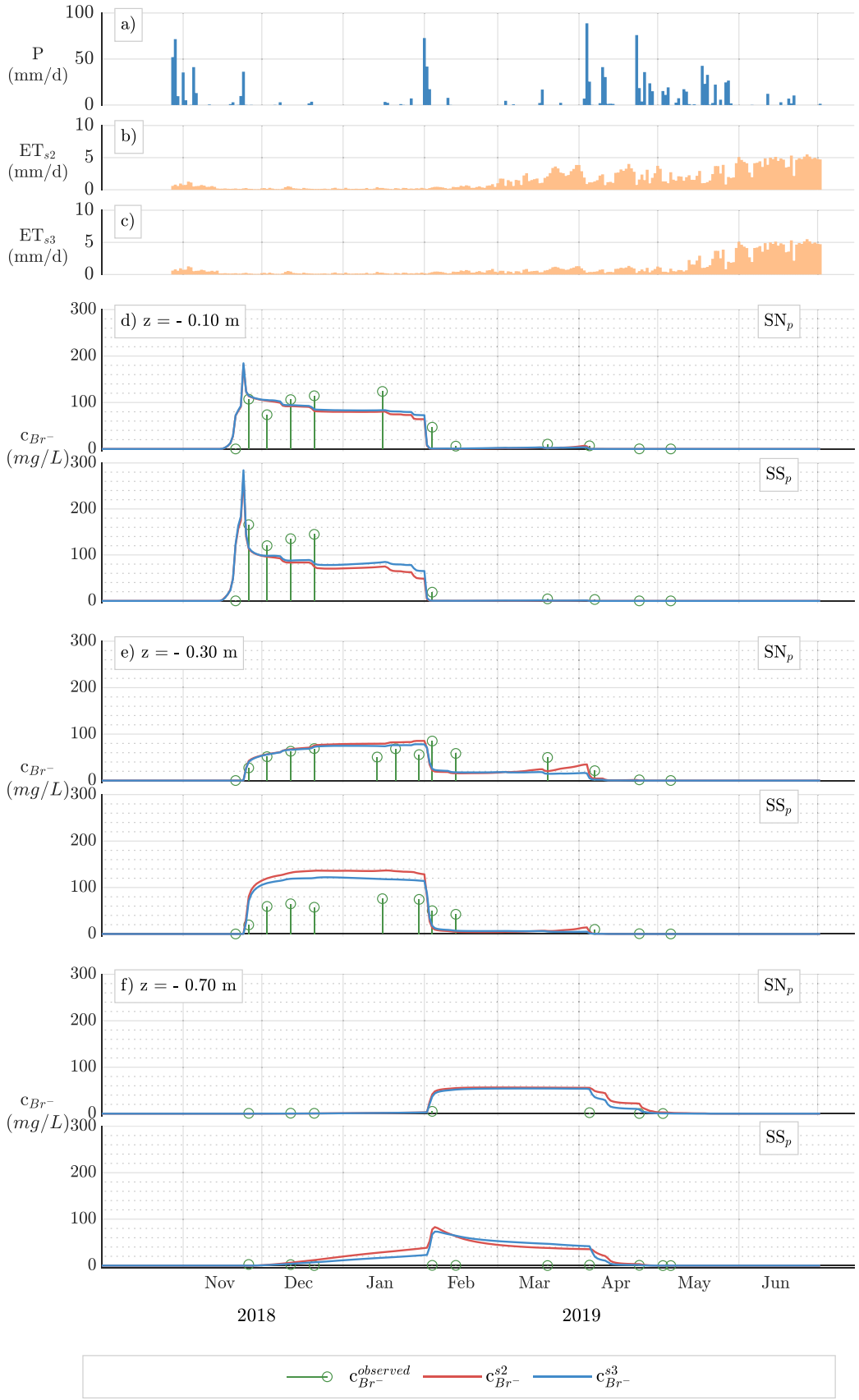

Fig. 7. Comparison between observed and simulated tracer concentration values at the Settolo site, along with rainfall and evapotranspiration forcing. Simulation results refer to scenarios s2 (red line) and s3 (blue line). (For interpretation of the references to color in this figure legend, the reader is referred to the web version of this article.)

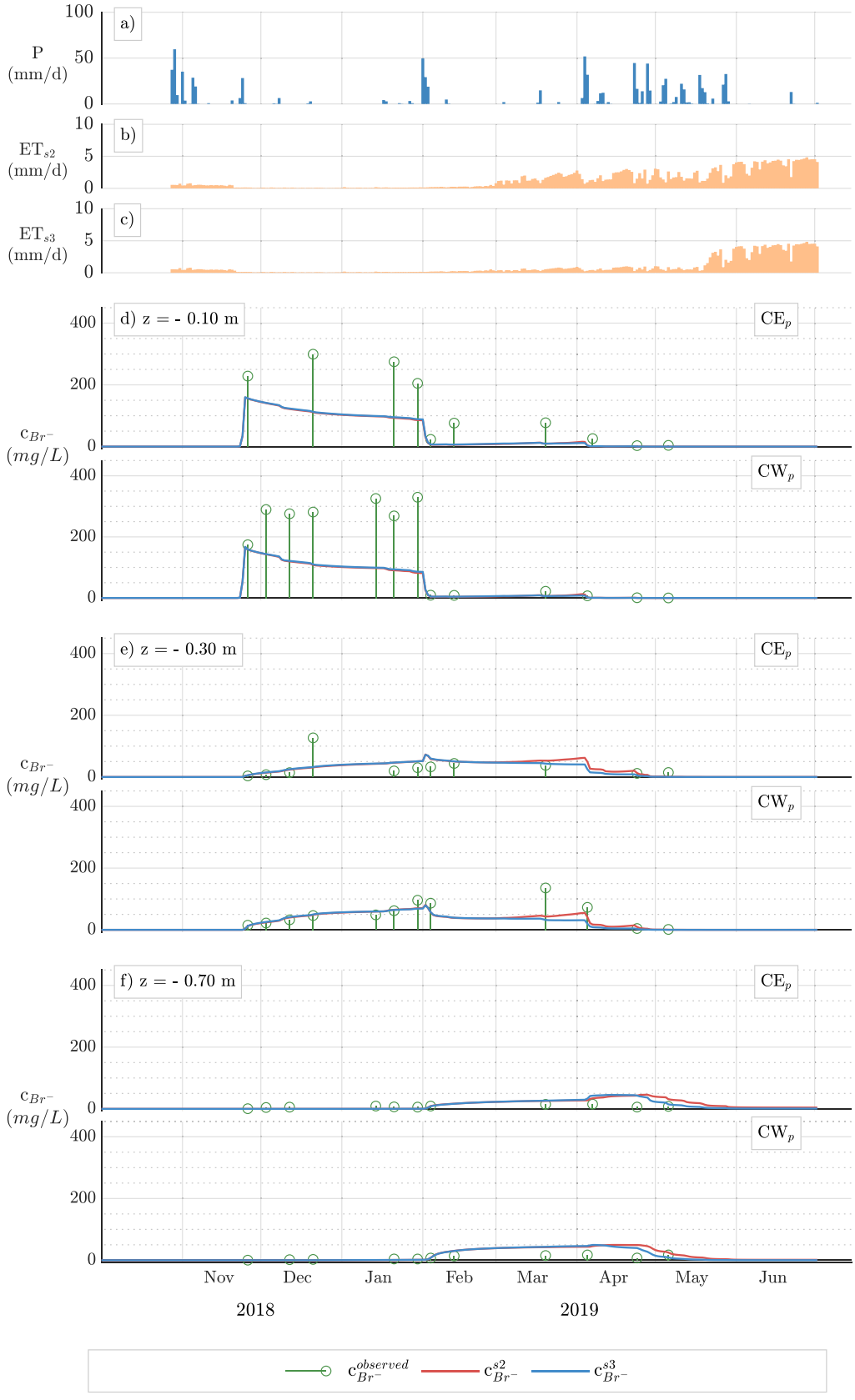

Fig. 8. Comparison between observed and simulated tracer concentration values at the Colnù site, along with rainfall and evapotranspiration forcing. Simulation results refer to scenarios s2 (red line) and s3 (blue line). (For interpretation of the references to color in this figure legend, the reader is referred to the web version of this article.)

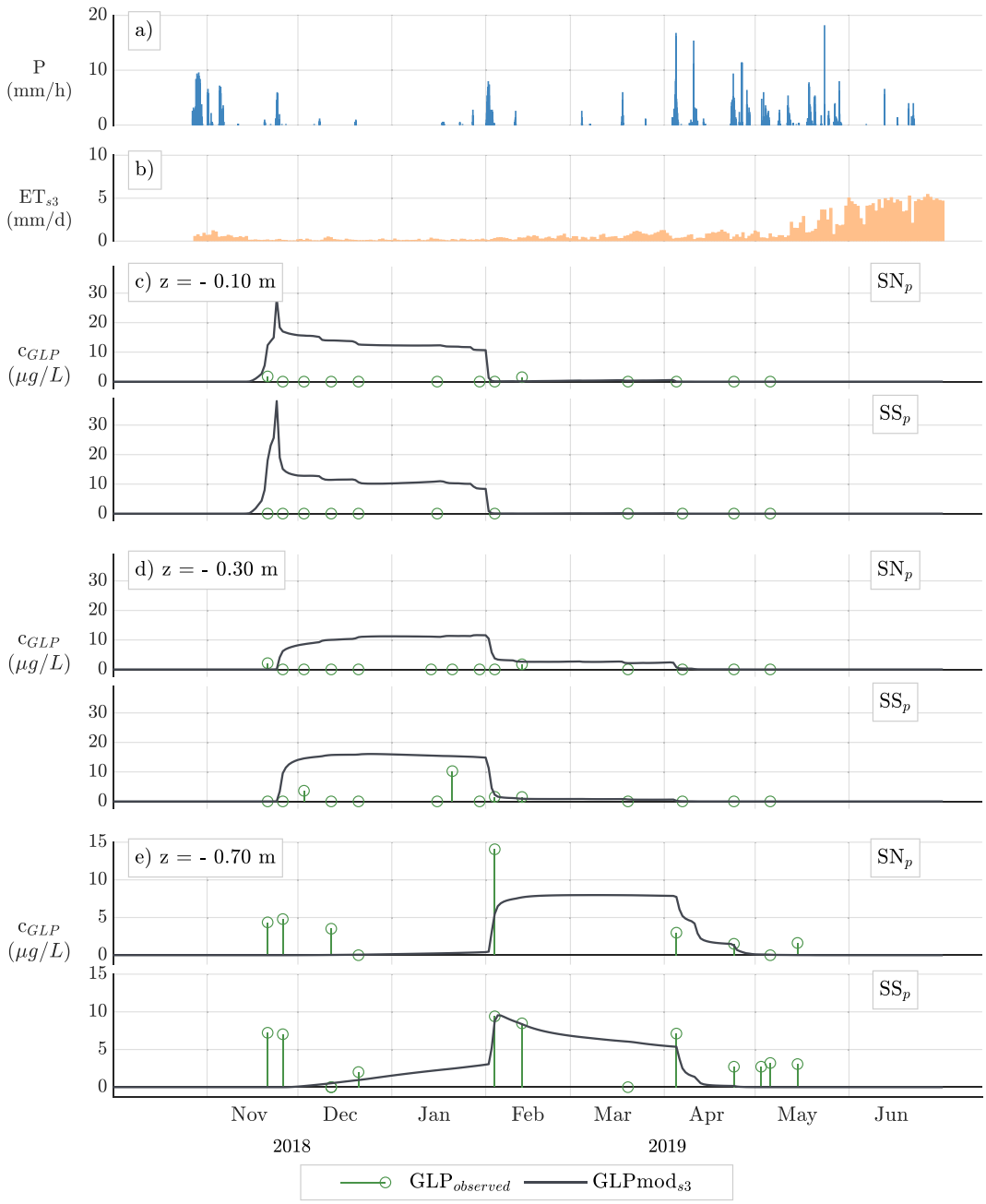

Fig. 9. Comparison between observed and simulated GLP concentration values at the Settolo site, along with rainfall and evapotranspiration forcing. Note the different vertical scale at −0.70 m, to better appreciate the reduced GLP concentration.

most cases inconsistent, in terms of timing and space, also if compared to the movement of the non-reactive tracer predicted by the advection–diffusion model. In the model, the GLP concentration in the infiltrating rainwater was related to the value of the soil-water partition coefficient K_d, whose values were derived from the GLP adsorption analyses carried out on the soil samples collected at each site plot. The use of plot-specific values of the coefficient in the simulations of the GLP evolution led to reasonable results in terms of maximum GLP concentrations. The reasonable results are limited to the unstructured first layer of soil in Colnù and to the bottom layer in Settolo, where the water samples were collected by the pan lysimeters. Probably due to different monitoring devices (porous cups), the lack of consistency between observed and modeled GLP concentration values in the remaining soil layers, hints at the combination of dissolved and particle-facilitated transport of the glyphosate. By the latter, the herbicide is adsorbed to the finest soil particles that, displaced by the most intense rainfall events, are transported through preferential pathways, while the remaining limited fraction is dissolved in the infiltrating rainwater.

In conclusion, the comparison between model and the field experimental evidence suggests that (i) one-dimensional analysis may be inadequate below the depth of 0.30 m ÷ 0.50 m, due to the soil heterogeneity and the presence of preferential flow-paths and (ii) the GLP infiltration in soils is also controlled by movement of the finest grains along macro-pores. Both considerations suggest the need to adopt, even at the small scale here considered, a more complex approach in the soil characterization, in the experimental data collection, and in the subsequent interpretative model. Geophysical surveys can give a more detailed description of soil heterogeneity, while a multiple pan lysimiter collection system may capture both dissolved and particle-facilitated (suspended) GLP fractions in the infiltrating rainwater. With

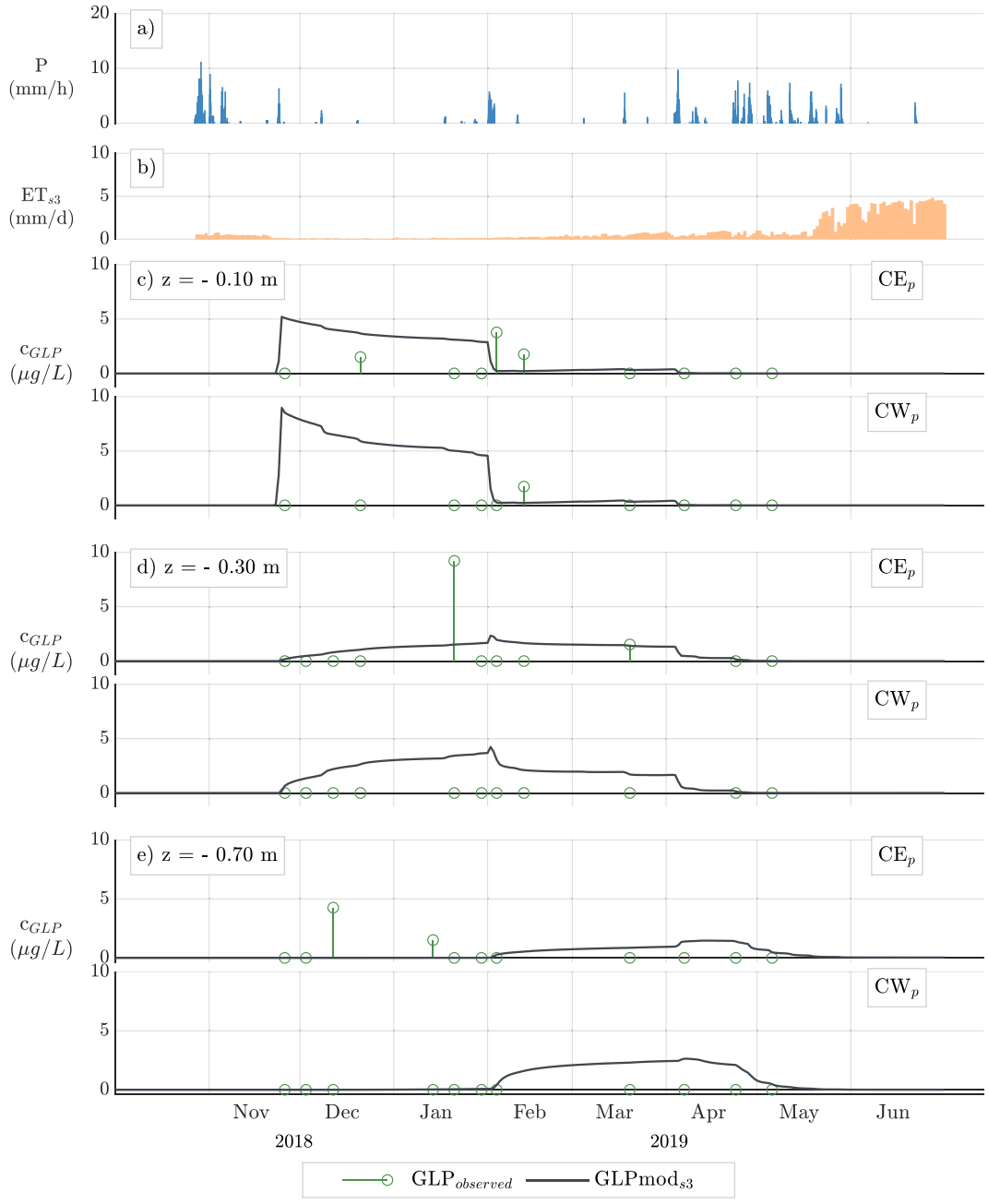

Fig. 10. Comparison between observed and simulated GLP concentration values at the Colnù site, along with rainfall and evapotranspiration forcing. Note the different vertical scale at −0.70 m, to better appreciate the reduced GLP concentration.

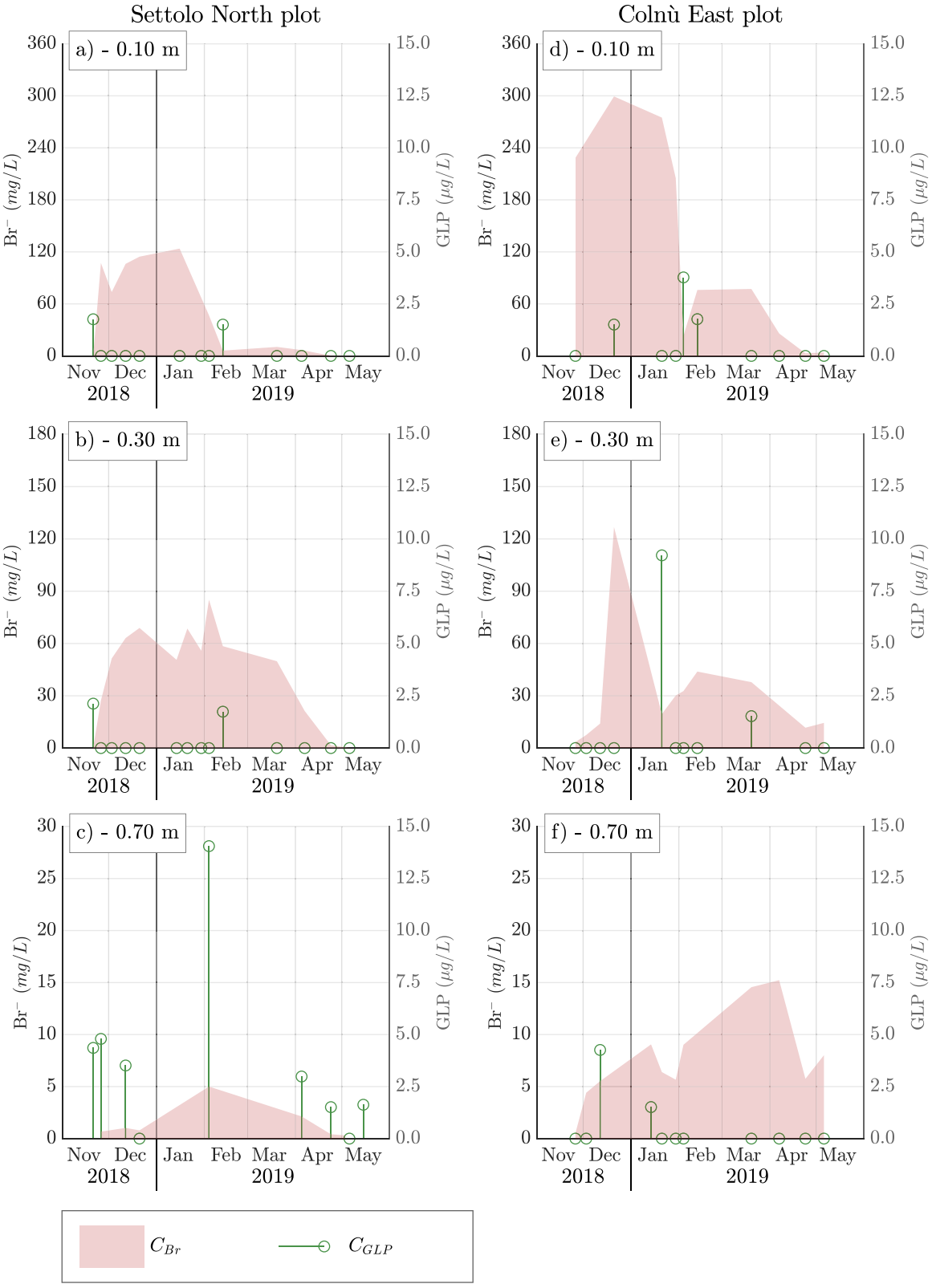

Fig. 11. Comparison between GLP and Br^- evolutions along the vertical in SN_p and in CE_p.

the data coming from a more complex experimental setup, one can go beyond the present first description obtained via one-dimensional analysis.

CRediT authorship contribution statement

Leonardo Costa: Conception and Design of the study, Formal analysis, Methodology. **Marta Mencaroni:** Data curation. **Nicola Dal Ferro:** Conception and Design of the study, Data curation. **Matteo Camporese:** Conception and Design of the study, Formal analysis, Methodology. **Francesco Morari:** Data curation. **Giuseppe Zanin:** Data curation. **Paolo Salandin:** Conception and Design of the study, Funding acquisition.

Declaration of competing interest

The authors declare that they have no known competing financial interests or personal relationships that could have appeared to influence the work reported in this paper.

Data availability

Data will be made available on request.

Acknowledgments

This study was carried out within the Uni-Impresa 2017 project SWAT (Sub-surface Water quality and Agricultural pracTices monitoring), developed by the Interdepartmental Research Center of Hydrology 'Dino Tonini' - University of Padova, together with the two integrated water-cycle management companies Alto Trevigiano Servizi and Piave Servizi. All authors contributed to the manuscript, and they have revised, read, and approved the submitted version.

Appendix A. Supplementary data

Supplementary material related to this article can be found online at https://doi.org/10.1016/j.jhydrol.2023.129886.

References

Allen, R.G., Pereira, L.S., Raes, D., Smith, M., et al., 1998. Crop Evapotranspiration-Guidelines for Computing Crop Water Requirements-FAO Irrigation and Drainage Paper 56, Vol. 300. Fao, Rome, p. D05109, (9).

Aparicio, V.C., De Gerónimo, E., Marino, D., Primost, J., Carriquiriborde, P., Costa, J.L., 2013. Environmental fate of glyphosate and aminomethylphosphonic acid in surface waters and soil of agricultural basins. Chemosphere 93 (9), 1866–1873. http://dx.doi.org/10.1016/j.chemosphere.2013.06.041.

Battaglin, W.A., Meyer, M.T., Kuivila, K.M., Dietze, J.E., 2014. Glyphosate and its degradation product AMPA occur frequently and widely in U.S. soils, surface water, groundwater, and precipitation. J. Am. Water Resour. Assoc. 50 (2), 275–290. http://dx.doi.org/10.1111/jawr.12159.

Baylis, A.D., 2000. Why glyphosate is a global herbicide: strengths, weaknesses and prospects. Pest Manage. Sci. 56 (4), 299–308. http://dx.doi.org/10.1002/(SICI)1526-4998(200004)56:4%3C299::AID-PS144%3E3.0.CO;2-K.

Bento, C.P., Commelin, M.C., Baartman, J.E., Yang, X., Peters, P., Mol, H.G., Ritsema, C.J., Geissen, V., 2018. Spatial glyphosate and AMPA redistribution on the soil surface driven by sediment transport processes a flume experiment. Environ. Pollut. 234, 1011–1020. http://dx.doi.org/10.1016/j.envpol.2017.12.003.

Borggaard, O.K., Gimsing, A.L., 2008. Fate of glyphosate in soil and the possibility of leaching to ground and surface waters: a review. Pest Manage. Sci. 64, 441–456. http://dx.doi.org/10.1002/ps.1512.

Carretta, L., Cardinali, A., Marotta, E., Zanin, G., Masin, R., 2019. A new rapid procedure for simultaneous determination of glyphosate and AMPA in water at sub μg/L level. J. Chromatogr. A 1600, 65–72. http://dx.doi.org/10.1016/j.chroma.2019.04.047.

Costa, L., Salandin, P., 2022. Wellhead protection areas vulnerability and the use of pesticides: the treviso province case study. Environ. Sci. Proc. 21 (1), http://dx.doi.org/10.3390/environsciproc2022021013.

Crestani, E., Camporese, M., Salandin, P., 2015. Assessment of hydraulic conductivity distributions through assimilation of travel time data from ERT-monitored tracer tests. Adv. Water Resour. 84, 23–36. http://dx.doi.org/10.1016/j.advwatres.2015.07.022.

Dal Ferro, N., Cocco, E., Lazzaro, B., Berti, A., Morari, F., 2016. Assessing the role of agri-environmental measures to enhance the environment in the veneto region, Italy, with a model-based approach. Agric. Ecosyst. Environ. 232, 312–325. http://dx.doi.org/10.1016/j.agee.2016.08.010.

Doherty, J.E., Hunt, R.J., 2010. Approaches To Highly Parameterized Inversion: A Guide To using PEST for Groundwater-Model Calibration, Vol. 2010. US Department of the Interior, US Geological Survey Reston.

Gupta, H.V., Kling, H., Yilmaz, K.K., Martinez, G.F., 2009. Decomposition of the mean squared error and NSE performance criteria: Implications for improving hydrological modelling. J. Hydrol. 377 (1–2), 80–91. http://dx.doi.org/10.1016/j.jhydrol.2009.08.003.

International Agency for Research on Cancer, 2017. Monographs on the evaluation of carcinogenic risks to humans 112, some organophosphate insecticides and herbicides. pp. 1–452.

Jarvis, N.J., 2007. A review of non-equilibrium water flow and solute transport in soil macropores: Principles, controlling factors and consequences for water quality. Eur. J. Soil Sci. (ISSN: 13510754) 58, 523–546. http://dx.doi.org/10.1111/j.1365-2389.2007.00915.x.

Kjær, J., Ernsten, V., Jacobsen, O.H., Hansen, N., de Jonge, L.W., Olsen, P., 2011. Transport modes and pathways of the strongly sorbing pesticides glyphosate and pendimethalin through structured drained soils. Chemosphere 84 (4), 471–479. http://dx.doi.org/10.1016/j.chemosphere.2011.03.029.

la Cecilia, D., Maggi, F., 2018. Analysis of glyphosate degradation in a soil microcosm. Environ. Pollut. 233, 201–207. http://dx.doi.org/10.1016/j.envpol.2017.10.017.

la Cecilia, D., Tang, F.H., Coleman, N.V., Conoley, C., Vervoort, R.W., Maggi, F., 2018. Glyphosate dispersion, degradation, and aquifer contamination in vineyards and wheat fields in the Po Valley, Italy. Water Res. 146, 37–54. http://dx.doi.org/10.1016/j.watres.2018.09.008.

Leon, M.E., Schinasi, L.H., Lebailly, P., Freeman, L.E.B., Nordby, K.C., Ferro, G., Monnereau, A., Brouwer, M., Tual, S., Baldi, I., Kjaerheim, K., Hofmann, J.N., Kristensen, P., Koutros, S., Straif, K., Kromhout, H., Schüz, J., 2019. Pesticide use and risk of non-hodgkin lymphoid malignancies in agricultural cohorts from France, Norway and the USA: A pooled analysis from the AGRICOH consortium. Int. J. Epidemiol. 48, 1519–1535. http://dx.doi.org/10.1093/ije/dyz017.

Maggi, F., 2019. BRTSim, a general-purpose computational solver for hydrological, biogeochemical, and ecosystem dynamics. arXiv:1903.07015.

Maggi, F., la Cecilia, D., Tang, F.H., McBratney, A., 2020. The global environmental hazard of glyphosate use. Sci. Total Environ. 717, 137167. http://dx.doi.org/10.1016/j.scitotenv.2020.137167.

Mencaroni, M., Cardinali, A., Costa, L., Morari, F., Salandin, P., Zanin, G., Dal Ferro, N., 2022. Glyphosate and AMPA have low mobility through different soil profiles of the Prosecco wine production area: a monitoring study in North-eastern Italy. Front. Environ. Sci. 1525. http://dx.doi.org/10.3389/fenvs.2022.971931.

Mencaroni, M., Longo, M., Cardinali, A., Lazzaro, B., Zanin, G., Ferro, N.D., Morari, F., 2023. Glyphosate and AMPA dynamics during the transition towards conservation agriculture: drivers under shallow groundwater conditions. Soil Tillage Res. (ISSN: 01671987) 229, 105659. http://dx.doi.org/10.1016/j.still.2023.105659.

Napoli, M., Marta, A.D., Zanchi, C.A., Orlandini, S., 2016. Transport of glyphosate and aminomethylphosphonic acid under two soil management practices in an Italian vineyard. J. Environ. Qual. 45 (5), 1713–1721. http://dx.doi.org/10.2134/jeq2016.02.0061.

Norgaard, T., Moldrup, P., Ferré, T.P., Olsen, P., Rosenbom, A.E., de Jonge, L.W., 2014. Leaching of glyphosate and aminomethylphosphonic acid from an agricultural field over a twelve-year period. Vadose Zone J. 13, http://dx.doi.org/10.2136/vzj2014.05.0054, vzj2014.05.0054.

Okada, E., Costa, J.L., Bedmar, F., 2016. Adsorption and mobility of glyphosate in different soils under no-till and conventional tillage. Geoderma 263, 78–85. http://dx.doi.org/10.1016/j.geoderma.2015.09.009.

Okada, E., Costa, J.L., Bedmar, F., Barbagelata, P., Irizar, A., Rampoldi, E.A., 2014. Effect of conventional and no-till practices on solute transport in long term field trials. Soil Tillage Res. 142, 8–14. http://dx.doi.org/10.1016/j.still.2014.04.002.

Peruzzo, P.J., Porta, A.A., Ronco, A.E., 2008. Levels of glyphosate in surface waters, sediments and soils associated with direct sowing soybean cultivation in north pampasic region of Argentina. Environ. Pollut. 156 (1), 61–66. http://dx.doi.org/10.1016/j.envpol.2008.01.015.

Pires Rosa, P.C., 2018. Brief review analytical methods for the determination of glyphosate. MOJ Toxicol. 4, http://dx.doi.org/10.15406/mojt.2018.04.00088.

Poiger, T., Buerge, I.J., Bächli, A., Müller, M.D., Balmer, M.E., 2017. Occurrence of the herbicide glyphosate and its metabolite AMPA in surface waters in Switzerland determined with on-line solid phase extraction LC-MS/MS. Environ. Sci. Pollut. Res. 24 (2), 1588–1596. http://dx.doi.org/10.1007/s11356-016-7835-2.

Richards, L.A., 1931. Capillary conduction of liquids through porous mediums. Physics 1, 318–333. http://dx.doi.org/10.1063/1.1745010.

Schaap, M.G., Leij, F.J., Van Genuchten, M.T., 2001. Rosetta: A computer program for estimating soil hydraulic parameters with hierarchical pedotransfer functions. J. Hydrol. 251 (3–4), 163–176. http://dx.doi.org/10.1016/S0022-1694(01)00466-8.

Silva, V., Montanarella, L., Jones, A., Fernández-Ugalde, O., Mol, H.G., Ritsema, C.J., Geissen, V., 2018. Distribution of glyphosate and aminomethylphosphonic acid (AMPA) in agricultural topsoils of the European union. Sci. Total Environ. 621, 1352–1359. http://dx.doi.org/10.1016/j.scitotenv.2017.10.093.

Starr, J., Paltineanu, I., 2002. Methods for measurement of soil water content: Capacitance devices. Methods Soil Anal.: Part 4.

Székács, A., Darvas, B., 2018. Re-registration challenges of glyphosate in the European Union. Front. Environ. Sci. 6 (July), 1–35. http://dx.doi.org/10.3389/fenvs.2018.00078.

Tang, F.H., Jeffries, T.C., Vervoort, R.W., Conoley, C., Coleman, N.V., Maggi, F., 2019. Microcosm experiments and kinetic modeling of glyphosate biodegradation in soils and sediments. Sci. Total Environ. 658, 105–115. http://dx.doi.org/10.1016/j.scitotenv.2018.12.179.

Todorovic, G.R., Rampazzo, N., Mentler, A., Blum, W.E., Eder, A., Strauss, P., 2014. Influence of soil tillage and erosion on the dispersion of glyphosate and aminomethylphosphonic acid in agricultural soils. Int. Agrophys. 28 (1), 93–100. http://dx.doi.org/10.2478/intag-2013-0031.

Trentin, T., 2021. Setup of Sensor Network and Modelling of the Aquifer System in the High Venetian Plain between Treviso, Padova and Venezia (Ph.D. thesis). University of Padova.

van Genuchten, M.T., 1980. A closed-form equation for predicting the hydraulic conductivity of unsaturated soils. Soil Sci. Am. J. 44 (5), 892–898. http://dx.doi.org/10.2136/sssaj1980.03615995004400050002x.

Yang, X., Wang, F., Bento, C.P., Xue, S., Gai, L., van Dam, R., Mol, H., Ritsema, C.J., Geissen, V., 2015. Short-term transport of glyphosate with erosion in Chinese loess soil — A flume experiment. Sci. Total Environ. 512–513, 406–414. http://dx.doi.org/10.1016/j.scitotenv.2015.01.071.